NUMERICAL CHARACTERIZATION OF THE EXCAVATION DAMAGED ZONE IN THE HG-A EXPERIMENT

Robert Walsh[1], Othman Nasir[1], Helen Leung[2], John Avis[1]

[1]*Geofirma Engineering Ltd, 1 Raymond Street, Ottawa, ON, Canada, K1G1R8, rwalsh@geofirma.com*
[2]*Nuclear Waste Management Organization, 22 St. Clair Ave. East,6th floor, Toronto, ON, Canada, M4T2S3*

The HG-A experiment, led by NAGRA from 2004 to the present, examined gas and water flow in the Excavation Damaged Zone (EDZ) of a tunnel in Opalinus clay. The experiment provided evidence for EDZ permeability changes due to swelling of the damaged rock in the presence of water and hydromechanical coupling following changes in pore and confining pressure. There is also evidence that low effective stress caused leakage of fluids along the packer-rock interface. Initially a two-phase flow model with variable EDZ permeability was used to model the system. This approach successfully reproduced pressure measurements in the HG-A test section. Modeling the gas injection tests did not require large changes in EDZ permeability, indicating that the EDZ properties were stabilizing at this stage of the test. We developed the T2GGM-FLAC model which simulates two-phase flow in T2GGM and mechanical processes in FLAC3D to model the EDZ. This coupled model predicted the development of EDZ around the HG-A tunnel, and then modeled the EDZ permeability as a function of time (self sealing) and packer pressure (hydromechanical coupling). The model predicted damage distribution around the HG-A tunnel corresponded well to available measurements of damage from post-excavation laser scans of the tunnel wall.

I. INTRODUCTION

Excavation of galleries, tunnels, and shafts in a waste repository inevitably causes disturbance and shifting of nearby host rock as the rock readjusts to the altered local stress regime. The properties of this excavation damaged zone (EDZ) around tunnels have become increasingly important to the performance assessment of nuclear waste repositories.

The HG-A field experiment at the Mont Terri underground research laboratory (URL) in Switzerland examined the long-term leakage of water and gas in the EDZ of a small, backfilled and sealed tunnel. This experiment identified the evolution, location, and properties of gas release pathways in a low permeability host rock (Opalinus clay). This modeling study was divided into two stages, first the HG-A test was simulated by a two-phase flow model for gas and water flow in the EDZ. Second, a coupled geomechanical model was developed to assess the extent and permeability of the EDZ. Of particular interest in all modeling stages was the temporal evolution of permeability in the system due to swelling of clay, and the effect of hydromechanical coupling on EDZ permeability.

II. EXPERIMENTAL DESCRIPTION

The horizontal HG-A tunnel is 13 m long and 1 m in diameter, excavated in the Mont-Terri URL (Figure. 1). The tunnel was drilled in a southwest direction along the strike of the bedding planes, which dip at a 45° angle towards the southeast. Further details are described in Ref. 1.

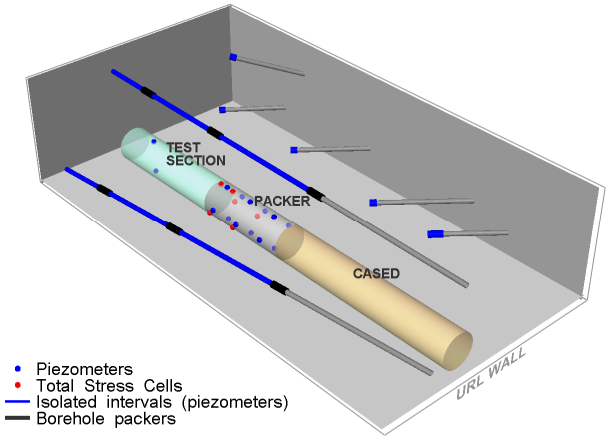

Fig. 1. Layout of the HG-A experiment showing piezometers and total stress sensors in and around HG-A.

The HG-A tunnel was divided into three sections. The deepest 4 m of the tunnel (from 9 - 13 m deep) is the test section into which water and gas were injected during the experiment. The test section was instrumented with piezometers, extensometers, strain gauges, time domain reflectometers, and geophones. After instrumentation, this section was backfilled with gravel behind a retaining wall. In the next 3 m section of the tunnel, from 6 - 9 m deep, a custom built "megapacker" was installed to seal the tunnel and hydraulically isolate the test section forcing escaping fluid to flow through the EDZ around the

packer. Instruments including piezometers and total stress cells were installed in this section between the packer and the tunnel wall. Following installation of the packer, the volume between the packer and the test-section retaining wall was filled with cement grout. The final 6 m of the tunnel was lined with a steel casing. A series of smaller boreholes were drilled into the surrounding rock and instrumented with piezometers and deformation gauges. Figure 1 shows a schematic of the HG-A experimental setup showing the locations of the total stress and fluid pressure sensors.

III. EXPERIMENTAL DATA SET

There is a substantial data set associated with the HG-A experiment. To develop and calibrate the models presented in this paper we relied largely on pore pressure and total stress measurements. Figure 2 shows a 2D projection of the total stress and fluid pressure sensors at the interface between the packer and the tunnel wall, for use in interpreting later figures.

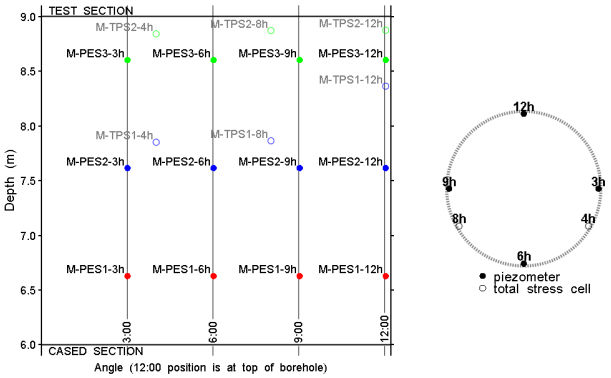

Fig. 2. 2D Projection of Sensor Locations at the Interface between the Packer and the Borehole Wall.

The packer was first inflated in November 2006. In 2007 a series of tests in which water was injected into the test section to saturate the test section with water and test the flow control units and the sensor array[2]. The backfill material was fully saturated by cycling water through the system to dissolve any trapped air. In January 2008 a multi-rate water injection test was started to investigate sealing phenomena in the EDZ in response to swelling of claystone, changes in total stress, and changes in pore pressure. This test continued for 750 days with varying water injection rates and packer pressures.

Figure 3 shows data from the multirate water injection test. Shown in the figure are measured pore pressure, measured total mechanical stress, and fluid injection rates in the test section. Higher injection rates led to higher pressures in the test section and along the outside of the packer. However, there was no unique correspondence between injection rate and pressure rise. The highest water injection rate (10 mL/min) occurred between 50 and 85 days, but the maximum pressure was observed at day 250, when the pumping rate was significantly lower (6 mL/min). This is best explained if the permeability of the EDZ is not constant. Increased packer pressure between days 127 and 273 compressed the EDZ, possibly reducing the permeability and causing increasing pressure in the test-section.

For a given change in pumping rate, the pressures in the test zone and adjacent to the packer changed rapidly, implying a low storage coefficient. After this rapid equilibration, a gradual, almost linear, pressure rise was observed, suggesting a continuous, gradual reduction in EDZ permeability. Large packer pressure changes are associated with small test section pore pressure changes, likely caused by changes in test section volume as the packer expands or contracts, deforming the test zone wall.

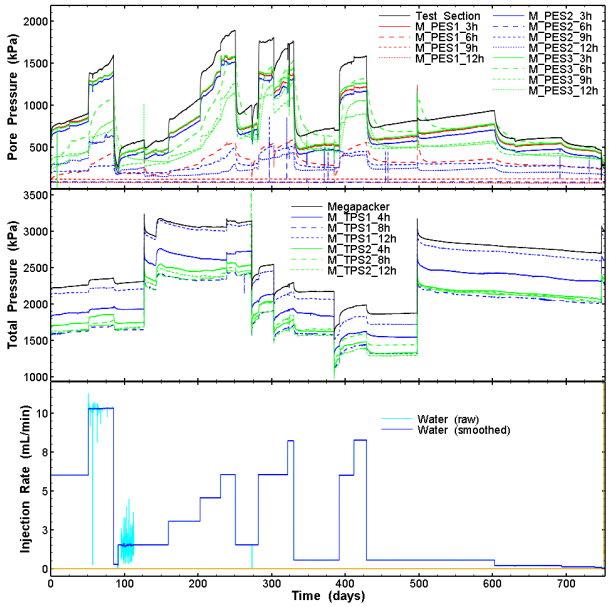

Fig. 3. Multirate Hydraulic Test Data from the HG-A Experiment. Time = 0.0 is Jan 23, 2008 at 12:00.

Figure 4 shows a 2D projection of pore pressures at the interface between the packer and the tunnel wall, arranged as shown in Figure 2, and showing evidence of a high permeability channel at roughly the 3 o'clock position on the tunnel wall. All sensors at the 3h position showed large and rapid responses to pressure change in the test zone; however, the lack of a pressure gradient along the channel suggests that this channel is not well connected to the atmospheric boundary[3]. There was also a pressure response between 9 and 12 o'clock with a roughly linear pressure gradient, indicating the existence of a second permeable channel connected to the atmospheric boundary behind the steel casing. The existence of these channels is consistent with observations of tunnel wall damage (see Figure 5).

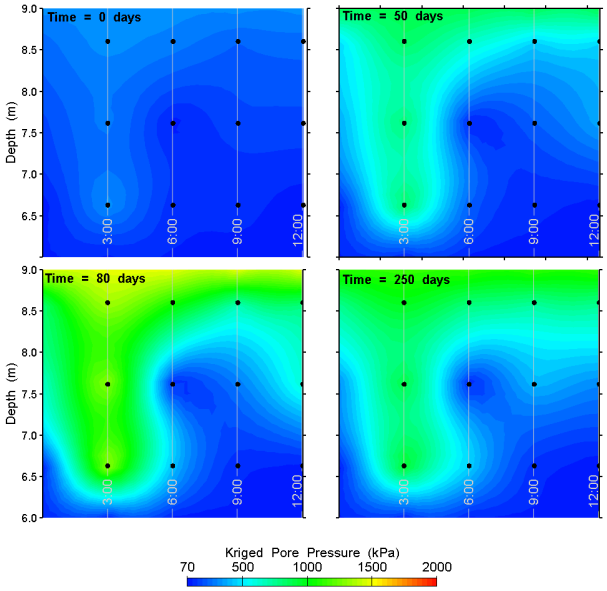

Fig. 4. 2D projection of pore pressures at the interface between the packer and the tunnel wall.

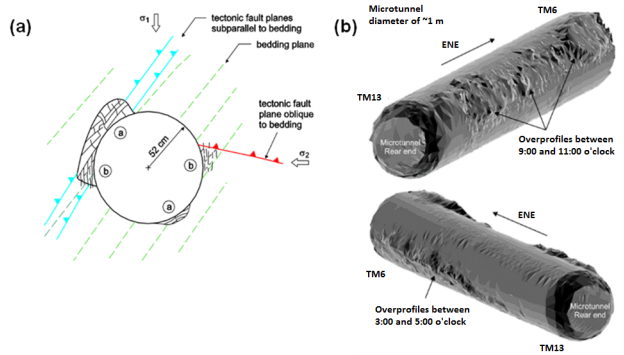

Fig. 5. Damage zone around tunnel (a) schematic representation and (b) laser scans of the tunnel wall.[4]

Figure 6 shows data from the three gas injection tests performed after the hydraulic test. The figure displays measured pore pressure and total mechanical stress at various locations in the HG-A tunnel, and fluid injection rates in the test section.

There is clear evidence for breakthrough of gas in tests Gas 2 and Gas 3. In both tests there is an inflection point after which gas pressure decays. This occurs without any changes in the pumping rate, and is likely caused by the development of a continuous gas filled pathway connecting to the atmosphere. Packer pressures were high and relatively stable during gas injection tests.

In Gas 2 and Gas 3, there are additional inflection points on the pressure curve. For instance, around day 1267 in Gas 3 the pumping rate dropped for 2 days. When pumping resumed at the same rate pressure rose to a new equilibrium. This may have been due to collapse of an unstable gas pathway when the injection rate dropped.

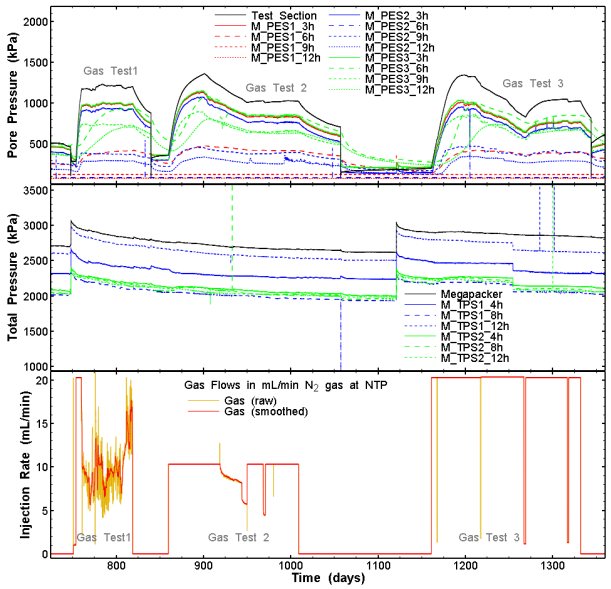

Fig. 6. Gas Injection Test Data from the HG-A Experiment. Time = 0.0 is Jan 23, 2008 at 12:00.

IV. MODELING THE EXPERIMENT

Modeling of the HG-A experiment was split into two phases: flow modelling and coupled hydromechanical modelling. The initial single and two-phase flow system modelling allowed simpler and more efficient model development, and a platform for testing conceptual models of the system. The flow models worked well to reproduce observed pressures, but they could not directly model the mechanical processes governing EDZ permeability. The hydromechanical model was developed subsequently to assess the impact of mechanical processes.

IV.A. Flow Modelling

The T2GGM code was used for the flow model. T2GGM combines the TOUGH2 two-phase flow code with a Gas Generation Model[5] and various other numeric and process enhancements. TOUGH2 is a general-purpose numerical simulation program for multi-phase fluid and heat flow developed by Lawrence Berkeley National Laboratory.[6] The EOS3 equation of state module used in T2GGM simulates the transport of a single gas phase in water. T2GGM allows for specification of alternate gases to air, the EOS3 default gas. EOS3 models the transport of dissolved gas in water by diffusion and advection. Dispersive processes are not modeled. Gas generation capabilities were not used.

To facilitate HG-A modeling, a function allowing time-dependent permeability specification was

implemented in T2GGM, allowing the user to select a subset of nodes and specify a tabular time dependent multiplier modifying the permeability at these nodes.

IV.A.1. Model Setup

A 3D radial model of the HG-A experiment was developed. The property distribution is shown in Figure 7. In the EDZ there are high permeability channels at the 3 and 9 o'clock positions to reflect what is believed to be high permeability channels at these locations. The channel at 3 o'clock is disconnected from the boundary. The channel permeability during the water injection tests was time-variable. The majority of external bondaries were set as no-flow boundaries, while the lower boundary at tunnel depth = 0 m and the end of the steel casing at depth = 6 m are constant pressure boundaries set to 101.3 kPa (1 atm).

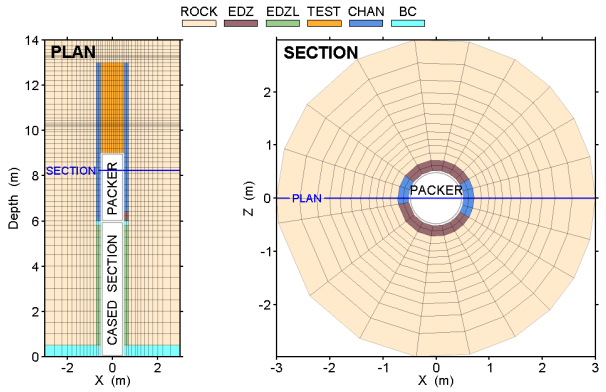

Fig. 7. 3D model discretization and property distribution.

The gas test models required increased test zone pore compressibility compared to the hydraulic test analysis, likely due to small volumes of gas trapped in the zone.

The permeable channel is caused by the presence of significant and connected fractures. In effect, this makes the channel EDZ a dual-porosity system in which the capillary pressure in the fractures would be significantly lower than that in the rock matrix.[7] To account for this, capillary pressure in the fractures was assumed to be equal to zero by setting the capillary pressure equal to zero below a certain gas saturation, which can be considered to equal the fracture pore volume. Through model calibration, setting capillary pressure to zero for water saturation above 0.985 was found to be generally optimal. This is equivalent to saying that the major permeable fractures comprise approximately 1.5 % of the EDZ pore volume. For gas saturation beyond 1.5% capillary pressure was based on van Genuchten equations.

IV.A.2. Time Varying Permeability

Initial runs used a constant EDZ permeability. This approach was inadequate, not accounting for the apparent swelling of Opalinus clay in contact with water or hydromechanical coupling.

To develop the time dependent permeability function, the rate of water injection and the resulting change in pressure was used. The test section was idealised as a closed volume with one inlet (the water injection valve) and one outlet (the EDZ). With this simplified model it was possible to solve for the bulk EDZ permeability. The resultant variable permeability curve for the multirate flow test is shown in Figure 8. Over the course of 750 days, there is a permeability drop that is slightly less than two orders of magnitude. After the 750 days the EDZ permeability remains 3 orders of magnitude higher than the estimated permeability of intact Opalinus clay.

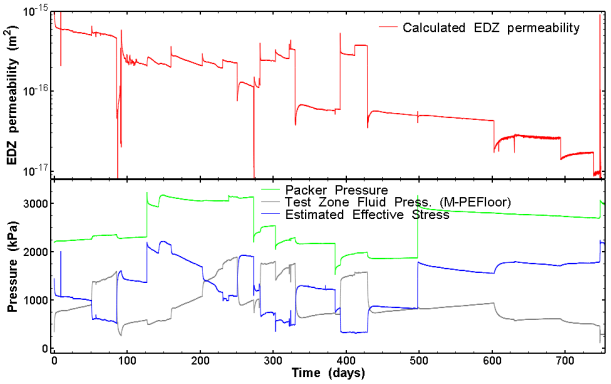

Fig. 8. EDZ permeability and contextual pressure data.

IV.A.3. Hydraulic Model Results

Figure 9 shows that using the time dependent permeability function resulted in a remarkable fit to the observed test zone pressure. A very simple conceptualisation of the HG-A system was able to reproduce experimental observations with good fidelity.

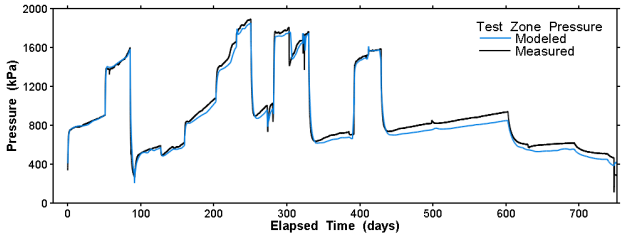

Fig. 9. Modeled test zone pressure during the multi-rate hydraulic test.

IV.A.4. Gas Test Model Results

All three gas injection tests followed similar patterns. Initially, the injected gas pools at the top of the test zone (see Figure 10) and remains largely trapped with a small amount of escaping into the EDZ directly above the gas pool. Eventually, the pool of gas reaches a depth where it

can enter the channel, quickly filling the fractures with gas. A continuous gas pathway connected to the boundary forms, and there is a pressure breakdown as gas leaves the test zone faster than it is injected.

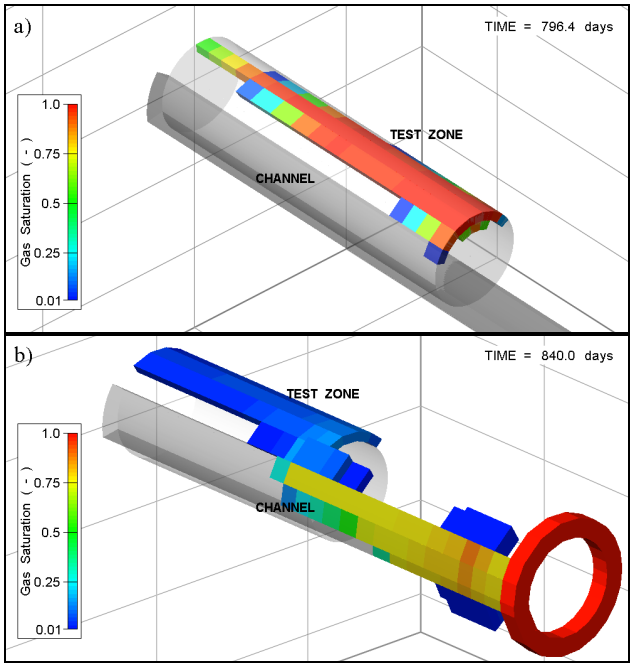

Fig. 10. Gas saturation showing a) close-up on test zone with gas pooled at the top, and b) gas saturation outside test zone with red ring representing atmospheric boundary.

Modeled test zone pressures for the gas tests are shown in Figure 11. For all three gas tests the model satisfactorily matched measured pressures. Gas Test 1 was modeled with a constant permeability. During this test only a minor amount of gas escaped the test zone and pressure was dissipated by displaced water escaping through the EDZ.

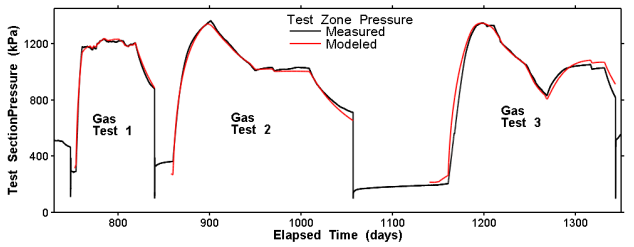

Fig. 11. Modeled test zone pressure during the gas tests.

The Gas Test 2 model also used a constant permeability. In Gas Test 2, the pressure rose until day 900, when there was a change in the trend and pressure began decreasing. At day 950, the pressure reached a steady state and pressure remained stable until gas shutoff at day 1009. The decline in test section pressure coincided with the formation of a continuous gas pathway through the channel allowing gas flow without displacing water.

Gas Tests 2 and 3 had approximately the same maximum pressure, and took the same amount of time to reach that pressure, despite the fact that the injection rate for Gas Test 3 was twice that of Gas Test 2. In order to reproduce this behaviour, test zone compressibility was raised by a factor of three. This suggests that a change occurred between the two tests, perhaps incomplete flushing of gas from the previous test.

In Gas Test 3 the constant permeability model overestimated pressure, and a time varying permeability was needed to match the pressure. At day 1247, the steepness of the pressure decay curve abruptly increased. There were no changes in packer pressure or pumping rate at this time, so this event has been interpreted as the development of a new connected gas pathway, and modeled by a small EDZ permeability increase. The test section pressure was on a downward trend when the gas injection stopped between days 1267 and 1269. When gas injection resumed at the same rate as before, pressure rose reaching a new equilibrium at a higher pressure. The cause may be an unstable gas pathway that closed during the two day gas injection interruption. This event was modeled as a small drop in permeability.

IV.B. Hydromechanical Modelling

Although the T2GGM models worked well to reproduce observed pressures, they could not model mechanical processes governing EDZ permeability. To allow this, the TOUGH-FLAC algorithm developed at LBL[8], which couples TOUGH2 and FLAC3D[9], was adapted to model the HG-A experiment. The hydromechanical (HM) modelling focused on the hydraulic testing stage, as this stage included the most interesting HM processes. Although the single-phase hydraulic test could be modeled with FLAC3D alone, this coupled tool was developed with future modelling of two-phase systems in mind. The gas tests were not modeled using the HM model as swelling processes were nearing completion, and packer pressures were constant. The fact that constant permeability models worked well for the gas tests implies that HM processes are no longer significant.

In this simulator, the modeling is controlled by T2GGM, which is responsible for solving flow processes. At each time step, the T2GGM model updates the pore pressure distribution and then calls a subroutine to pass updated pressures to and then run FLAC3D. The updated pore pressures change the effective stresses causing a new equilibrium stress state. FLAC3D assesses the resulting deformation and damage. Damage and stress information is returned to T2GGM for update of permeability, and flow solution resumes. This approach allows simulation of permeability due to excavation damage, changes in pore pressure, and changes in applied stress. Other

processes included in the model are swelling (time dependent) and leakage around the packer (as a function of effective stress at the packer-rock interface).

To model tunnel EDZ development the Ubiquitous-Joint Model (UJM) was used.[9] This model accounts for the elasto-plastic behaviour of the anisotropic (bedded) Opalinus clay by modelling it as a Mohr-Coulomb solid with weak planes at a specific orientation.

The UJM provides the extent of the damaged zone. The permeability of this damaged zone must be calculated using an empirical function to connect damage and effective stress to permeability. This function was calibrated by comparing model predictions of test zone pressure to experimentally determined values. The form of the proposed equation is as follows:

$$\log k_d = A + Be^{C\sigma'_{avg}} \qquad (1)$$

Where σ'_{avg} is average effective stress (Pa)

A, B, and C are fitting parameters

k_d is the damaged zone permeability (m^2)

Parameter A represents residual permeability present at high stresses. Parameter B controls the post-damage permeability increase when confining stress declines to zero and is higher where multiple failure modes coincide. Parameter C controls the slope of the permeability-stress relationship. The form of Eq. (1) is similar to that suggested by Ref.10 and authors studying basin scale or subglacial compaction.[11,12] It is also in agreement with laboratory scale measurements of stress-permeability coupling in single fractures.[13,14]

In the Opalinus clay, there is ample evidence that permeability may be reduced through self-sealing, primarily due to swelling of the fracture wall material.[3,15] The permeability change as a result of swelling (self-healing of damage zone) is modeled as exponential decay with time, introducing another calibration parameter (D).

$$k = k_d e^{D(t-t_0)} \qquad (2)$$

In laboratory-scale samples of Opalinus clay, time and stress dependent evolution of permeability have been studied.[16] These experimental results could be modeled using Eq. (1) and (2), showing behavior consistent with this mathematical approach.

The packer was installed to force any fluid leaking from the test zone through the EDZ. During the hydraulic test there were two times when the test zone pressure approached or surpassed the applied stress at the packer-rock interface. These correspond to times of elevated apparent EDZ permeability based on the analysis described in Section IV.A.2, suggesting that water is leaking along the interface. The packer-wall interface is akin to a fracture, so a log-linear permeability-stress function was used to calculate permeability of this interface, allowing fluid to escape when effective stress is low.

IV.B.1. Model Setup

The Opalinus Clay at Mont Terri is a slightly over-consolidated rock with reduced shearing resistance along steeply dipping bedding planes.[17] This is incorporated into our geomechanical conceptual model by using the UJM with input parameters from laboratory and in-situ tests.[4]

T2GGM-FLAC modelling was carried out using a radially gridded 3D block model. The T2GGM and FLAC models used similar grids with identical elemental centroids. The domain has dimensions of 20 m × 18 m × 20 m, centered on the tunnel. Figure 12 shows a cut-away section halfway through the model domain. The presence of nearby access tunnels is neglected in the model.

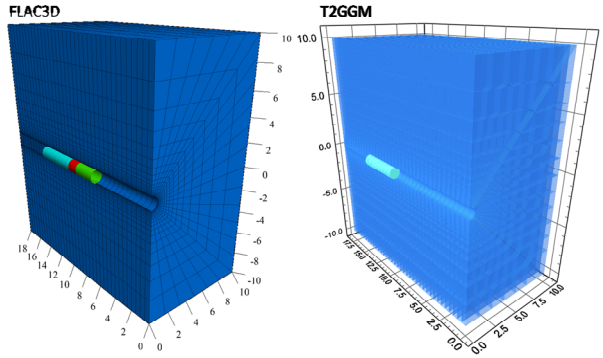

Fig. 12. Cut-away cross section through model domain, comparing FLAC3D and TOUGH2 geometry.

The local principle stresses are estimated to be 6.5 MPa oriented vertically, 2.5 MPa oriented horizontally parallel to the tunnel, and 4.5 MPa oriented horizontally perpendicular to the tunnel.[2,18] For the packer-rock interface, a specified stress boundary condition normal to the tunnel surface and divided into two zones with different applied stresses was applied.

IV.B.2. Model Results

The extent of the EDZ was evaluated based on the plastic failure state from the UJM. Figure 13 shows the model predicted bedding plane shear and tension failure zones. This can be compared to laser scan of the tunnel performed following the excavation (Figure 5). Results show good agreement between model and observation. The locations where failure modes overlap correspond to measured breakout locations.

Generalizing from this model, if pore pressure were sufficiently high, this could enhance and expand the EDZ. Stresses applied to the tunnel wall, such as the packer pressure, partially support the wall and reduce the degree of damage and the permeability. The action of the packer

in the HG-A experiment is somewhat analogous to the effect of a swelling clay-based seal in a repository setting.

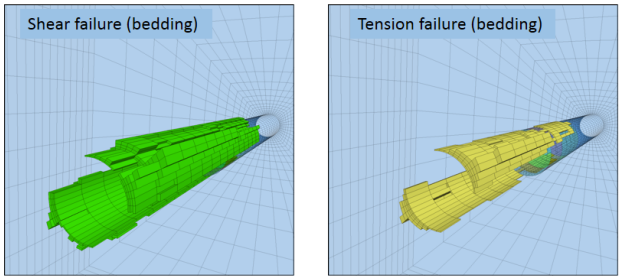

Fig. 13. Failure modes delineating the EDZ extents.

Figure 14 shows a cross section through the tunnel. The left panel shows the estimated extent of the damage zone resulting from the combination of all failure modes. The modeled damage zone is similar in both orientation and extent to the schematic representation of the damage zone in Figure 5. The right panel shows the estimated EDZ permeability. Where multiple modes of failure are predicted the permeability increase is greater. The EDZ permeability is a function of effective stress and time dependent permeability decay (swelling); therefore, it changes during the simulation.

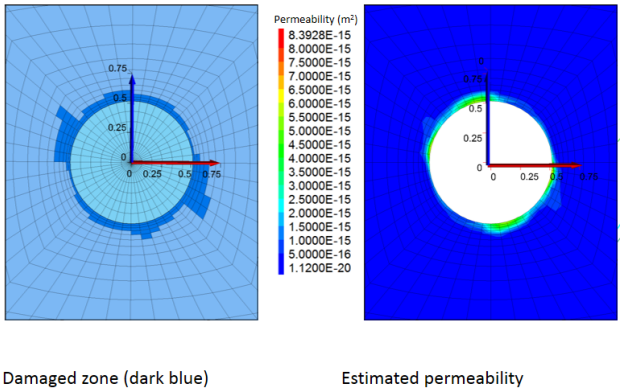

Fig. 14. Damaged zone and estimated permeability.

In Figure 15 simulated pressures during the multi-rate hydraulic test are compared to measurements. In general, the simulated and measured pressures compare well. More time spent on parametric fitting could improve this result.

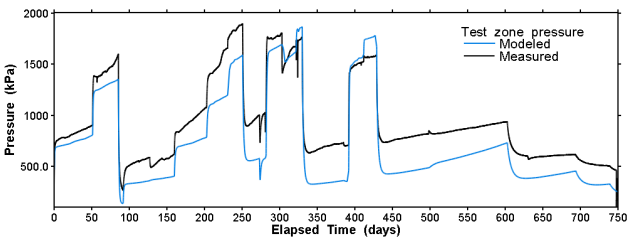

Fig. 15. Modeled test zone pressure during the multi-rate hydraulic test.

The permeability of the EDZ controls the test zone pressure, and all key processes should be considered when modeling the evolution of the EDZ. First, we used the rock mechanical model to calculate the extent and degree of damage in the rock surrounding the tunnel. This analysis was based on laboratory measurements of rock properties, and on credible estimates of the in-situ stress tensor. The damage distribution calculation used parameters independent of the field test, and resulted in a damage distribution, qualitatively similar to the breakout distribution from laser-scans of the tunnel interior.

There is currently no generally applicable rule to convert damage to permeability. To calculate the induced permeability of the EDZ, it was necessary to calibrate the damage-permeability equation. Permeability of the EDZ is not only a function of damage. As the packer pressure and test zone pressures changed during the test, the effective stress and thus the permeability of fractures in the EDZ also changed. Stress-permeability coupling is difficult to determine a priori, as it is a function of fracture geometry, failure mode, mechanical restraints, and basic rock mechanical properties. The permeability of single fractures in laboratory test specimens varies widely, even in rocks with similar bulk elastic properties. In general, however, fractures become stiffer at increasing confining stresses, reducing the degree of fracture wall deformation and the resulting changes in permeability for a given stress increment. The exponential form of Eq. (1) reflects this generally expected behavior.

Finally, the evolution of the EDZ due to swelling and self-healing of the fracture walls was included in the model. An exponential decay function for reducing permeability with time has been observed in laboratory-scale experiments, and this form was adopted for Eq. (2). Combining these functions, the EDZ permeability produced a reasonably good fit to the test zone pressures.

V. CONCLUSIONS

Initial modelling using T2GGM showed that the experimental results of the hydraulic test (from January 2008 to April 2010) cannot be reproduced using a constant EDZ permeability. The permeability of the EDZ during the first 839 days of the HG-A experiment was variable and affected by two distinct processes: (1) fracture healing by swelling of the damaged rock in the presence of water which resulted in a steady reduction in the permeability; and (2) HM coupling in response to changes in pore pressure and packer pressure.

Two approaches for estimating the changes in permeability during the hydraulic test were developed. The first approach was to back-calculate permeability as a function of pressure change. This approach provided a good fit to modeled pressures, but is not predictive. By the end of the multi-rate hydraulic test, the properties of

the EDZ were approaching a steady state. The Gas Tests were modeled using constant EDZ permeability.

The second approach to estimating the EDZ permeability is the coupled HM approach, in which the EDZ development is a function of plastic deformation and EDZ permeability is based on an empirical stress-permeability coupling relationship. This approach is considered predictive in terms of modelling the extent and geometry of the EDZ. Calculation of the damage-induced permeability required calibration of a number of empirical parameters. With limited calibration, this approach reproduced measured test zone pressures reasonably well.

The EDZ predicted by the hydromechanical model is relatively thin and heterogeneous. Permeability is not uniformly distributed around the circumference of the tunnel, but localized in channels. The extent of the EDZ is very much a function of the magnitudes and orientation of the local stress tensor and the fabric of the rock. While this model used a homogenous (and anisotropic) distribution of stresses and rock properties, it produced a heterogeneous EDZ. Local variations in stress or rock fabric would further amplify EDZ heterogeneity.

ACKNOWLEDGMENTS

We gratefully acknowledge the Nuclear Waste Management Organization for supporting this work. Thank you to Jonny Rutqvist for providing us the TOUGH-FLAC algorithm which saved us a great deal of time in developing our coupling algorithm.

REFERENCES

1. O. MEIER, C. NUSSBAUM, and P. BOSSART. *HG-A Experiment: Drilling of the Microtunnel (BHG-A0 and BHG-A1). Mont Terri Project Technical Note 2005-55,* Geotechnical Institute Ltd., St. Ursanne, Switzerland (2005).
2. G.W. LANYON, P. MARSCHALL, T. TRICK, R. DE LA VAISSIERE, H. SHAO and H. LEUNG. "Hydromechanical Evolution and Self-Sealing of Damage Zones around a Microtunnel in a Claystone Formation of the Swiss Jura Mountains," *The 43rd US Rock Mechanics Symposium and 4th U.S.-Canada Rock Mechanics Symposium*, Asheville, NC, June 28 to July 1, 2009, American Rock Mechanics Association (2009).
3. G.W. LANYON. *HG-A (Gas Path Through Host Rock and Along Seals) Experiment: Preliminary Interpretation of Gas Injections during Phase 15 &16.* Mont Terri TN 2010-40. Fracture Systems Ltd, St Ives, Cornwall, United Kingdom (2012).
4. P. MARSCHALL, M. DISTINGUIN, H. SHAO, P. BOSSART, C. ENACHESCU and T. TRICK. "Creation and Evolution of Damage Zones around a Microtunnel in a Claystone Formation of the Swiss Jura Mountains." *The 2006 SPE International Symposium and Exhibition on Formation Damage Control,* Lafayette, L.A., 15–17 February 2006, SPE Paper 98537.
5. P. SUCKLING, J. AVIS, N. CALDER, P. HUMPHREYS, F. KING and R. WALSH. *T2GGM Version 3.1: Gas generation and Transport Code, NWMO TR-2012-23*. Nuclear Waste Management Organization, Toronto, Canada (2012).
6. K. PRUESS, C. OLDENBURG and G. MORIDIS. *TOUGH2 User's Guide, Version 2.0*. Lawrence Berkeley National Laboratory LBNL-43134. Berkeley, USA (1999).
7. L. ZHANG, and D. G. FREDLUND. "Characteristics of Water Retention Curves for Unsaturated Fractured Rocks." *The Second Asian Conference on Unsaturated Soils*, Osaka, Japan, April 15-17, 2003, UNSAT-ASIA (2003).
8. J. RUTQVIST, and C.F. TSANG. "TOUGH-FLAC: A Numerical Simulator for Analysis of Coupled Thermal-Hydrologic-Mechanical Processes in Fractured and Porous Geological Media under Multi-phase Flow Conditions." *TOUGH2 Symposium 2003*, May 2003, Lawrence Berkeley National Laboratory, Berkeley, California (2003).
9. ITASCA CONSULTING GROUP INC. *FLAC3D (Fast Lagrangian Analysis of Continua). V.5.01,* Itasca Consulting Group, Minneapolis, MN (2012).
10. T. POPP, K. SALZER and W. MINKLEY. *Physics and Chemistry of the Earth,* **33**, S374-S387 (2008).
11. C.M. BETHKE and T.F. CORBET. *Water Resources Research*, **24**, 461–467 (1988).
12. M. PERSON, V. BENSE, D. COHEN and A. BANERJEE. *Geofluids*, **12**, 58-78 (2012).
13. R. WALSH, C. MCDERMOTT and O. KOLDITZ. *Hydrogeology Journal*, **16,** 4, 613-627 (2008).
14. C. DAVY, F. SKOCZYLAS, J.D. BARNICHON and P. LEBON. *Physics and Chemistry of the Earth* **32**, 667-680 (2007).
15. H. BOCK, B. DEHANDSCHUTTER, C. D. MARTIN, M. MAZUREK, A. DE HALLER, F. SKOCZYLAS and C. DAVY. *Self-sealing of Fractures in Argillaceous Formations in the Context of Geological Disposal of Radioactive Waste Review and Synthesis Report OECD NEA 6184*, OECD, Paris, France (2010).
16. F. BERNIER, X.L. LI, W. BASTIAENS, L. ORTIZ and M. VAN GEET. *SELFRAC – Fractures and Self-healing within the Excavation Disturbed Zone in Clays – Final Report. 5th EURATOM Framework Programme*, EU-Commission , Brussels (2007).
17. C.D. MARTIN and G.W. LANYON. *Int. J. Rock Mech. Min. Sci*., **40**, 7-8, 1077-1088 (2003).
18. A.G. CORKUM and C.D. MARTIN. *Int. J. Rock Mech. Min. Sci.*, **44**, 846-885 (2007).